GEORGIA INSTITUTE OF TECHNOLOGY — OFFICE OF CONTRACT ADMINISTRATION

PROJECT ADMINISTRATION DATA SHEET

[x] ORIGINAL
[ ] REVISION NO. ____

Project No. A-2996 DATE: 7/28/81

Project Director: Dr. B. R. Livesay ~~School~~/Lab EML/PSD

Sponsor: CILCO, Inc.; Huntington, W. Va. 25717

Type Agreement: Purchase Order No. 80-1833

Award Period: From 6/16/81 To 8/15/81 (Performance) ----- (Reports)

Sponsor Amount: $4,500 Contracted through:

Cost Sharing: none (GTRI) ~~GTRI~~

Title: Determining Strength and Stress Parameters For CILCO SK-1 Intraocular Lenses

ADMINISTRATIVE DATA OCA CONTACT Duane Hutchison x4820

1) Sponsor Technical Contact: Mr. Richard Johnson; CILCO, Inc.; P.O. Box 218; Lesage, W.V. 25537 304-736-5239

2) Sponsor Admin./Contractual Contact: Terry Higgins, Purchasing Agent; CILCO, Inc.; P.O. Box 1680; Huntington, W.V. 25717

Reports: See Deliverable Schedule Security Classification: none

Defense Priority Rating: none

RESTRICTIONS

See Attached N/A Supplemental Information Sheet for Additional Requireme

Travel: Foreign travel must have prior approval - Contact OCA in each case. Domestic travel requires sponsor approval where total will exceed greater of $500 or 125% of approved proposal budget category.

Equipment: Title vests with N/A

COMMENTS:

COPIES TO:

Administrative Coordinator
Research Property Management
Accounting Office
Research Security Services
✓ Reports Coordinator (OCA)
Legal Services (OCA)
EES Research Public Relatic
Project File (OCA)
Other:

GEORGIA INSTITUTE OF TECHNOLOGY OFFICE OF CONTRACT ADMINISTRATION

SPONSORED PROJECT TERMINATION/CLOSEOUT SHEET

Date December 5, 1983

Project No. A-2996 ~~School~~/Lab EML

Includes Subproject No.(s) _____

Project Director(s) Dr. Billy R. Livesay GTRI / ~~GTRI~~

Sponsor CILCO, Inc.

Title Determining Strength and Stress Parameters for CILCO SK-1 Intraocular Lenses

Effective Completion Date: 8/15/81 (Performance) 8/15/81 (Reports)

Grant/Contract Closeout Actions Remaining:

- [ ] None
- [X] Final Invoice ~~or Final Close-Out Report~~
- [ ] Closing Documents
- [ ] Final Report of Inventions
- [ ] Govt. Property Inventory & Related Certificate
- [ ] Classified Material Certificate
- [ ] Other _____

Continues Project No. _____ Continued by Project No. _____

COPIES TO:

Project Director
Research Administrative Network
Research Property Management
Accounting
Procurement/EES Supply Services
Research Security Services
Reports Coordinator (OCA) ✓
Legal Services
Library
GTRI
Research Communications (2)
Project File
Other _____

A-2996
Final Report

MICROMECHANICS MEASUREMENTS OF INTRAOCULAR LENS STRENGTH AND STRESS PARAMETERS

BY

B.R. LIVESAY

MICROMECHANICS LABORATORY
PHYSICAL SCIENCES DIVISION

GEORGIA INSTITUTE OF TECHNOLOGY
ATLANTA, GEORGIA 30332

Prepared For

CILCO, Inc.

HUNTINGTON, WEST VIRGINIA

July 9, 1981

INTRAOCULAR LENS STRENGTH AND STRESS PARAMETERS

Introduction

This report is concerned with the results of mechanical property tests conducted at the Georgia Institute of Technology on CILCO SK-1 intraocular lens specimens manufactured by CILCO, Inc. of Huntington, West Virginia. Mr. Richard Johnson of CILCO visited Georgia Tech on June 12, 1981 to discuss the three types of mechanical tests needed to satisfy both Federal regulations and CILCO imposed quality control requirements. Similar work on other types of intraocular lenses had been conducted elsewhere, apparently employing the commercial testing machines normally used for structural materials. Mr. Johnson was aware of the Micromechanics Laboratory which was developed at Georgia Tech specifically to accommodate mechanical property investigations on very small specimens. One of the instruments of the Micromechanics Laboratory proved to be well suited for conducting the intraocular lens tests outlined by Mr. Johnson.

Mechanical tests were desired under the following three modes of deformation:

A. Diagonal Compression

B. Loop Tensile Strength

C. Vertical Compression, or Shear.

The deformation modes are schematically illustrated in Figures 1-3. The lenses were all plano-convex with a diameter of about 6 mm and a thickness of about 0.8 mm. There is a distance of about 13 mm between the two holes at the ends of the two loops. The diameter of the fine fiber-like loop itself is about 0.09 mm.

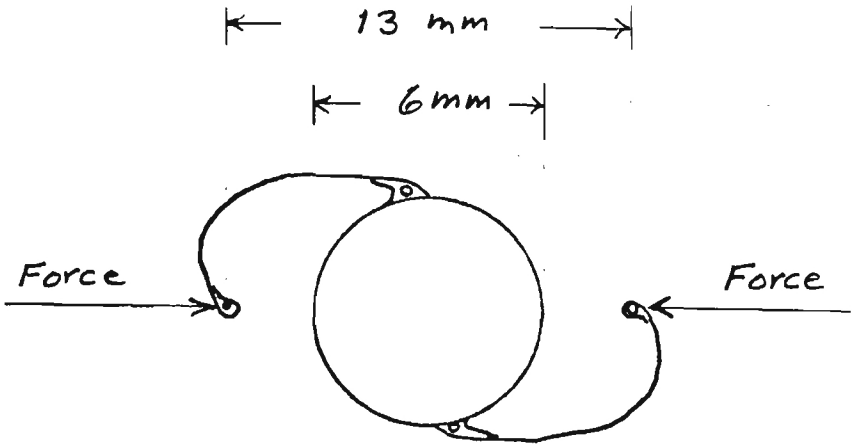

Figure 1. Schematic of Diagonal Compression Test Geometry

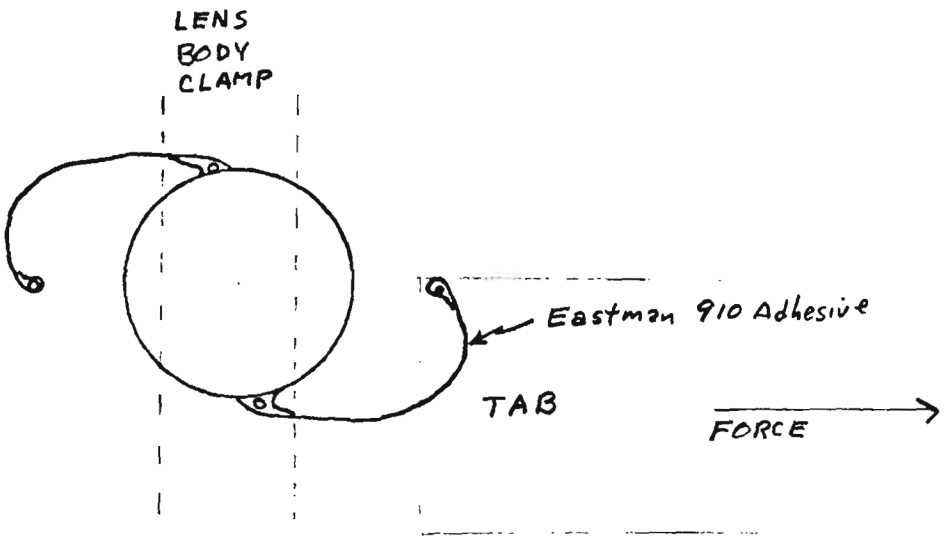

Figure 2. Schematic of Loop Tensile Strength Test Geometry

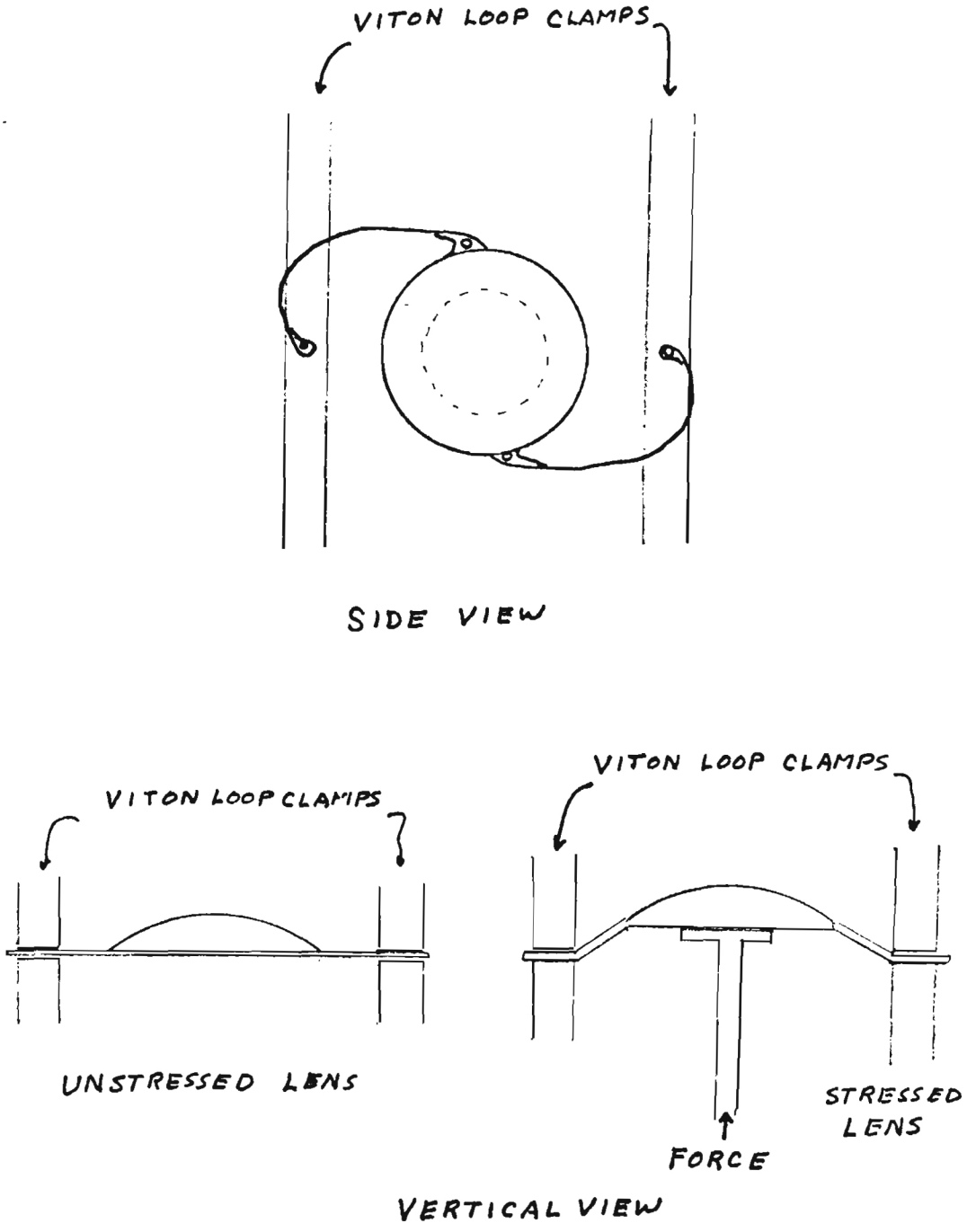

Figure 3. Schematic of Compressive Shear Test Geometry

Experimental

A photograph of the micromechanical testing apparatus employed for these measurements is shown in Figure 4. Two force transducers found to be suited to the loads involved with these lens models were a 0 to $\pm$ 450 gram-force device based on a differential transformer and a 0 to $\pm$ 30 gram force device based on a precision strain gage. The larger loadcell is shown installed in Figure 4. Specimen elongation was measured with a differential transformer device. The electronic circuitry for the transducers and other controls is seen on the shelf at the upper right in (and out of) the photograph. Force-elongation curves were thus plotted directly as lens specimens were stressed on the x-y plotter seen just behind the test apparatus. A binocular microscope with a zoom capability and a calibrated eye piece is mounted directly above the test fixtures to aid in mounting specimens and for observations of deformation during tests. Synchronous motors are used to drive a micrometer screw for elongating test specimens on this apparatus. A displacement rate of 1.058×10^{-2} mm/sec was decided to be best suited for these measurements. All but some 2 or 3 specimens were elongated at this rate.

Special fixtures were needed for each of the three deformation modes. The configuration of an intraocular lens is, of course, quite different from that of normal mechanical test specimens. However, the testing machines in this laboratory were all designed to accommodate a wide variability in both test fixtures and environments.

The simple test fixtures employed with the diagonal compression tests are shown in photographs of Figure 5. The specimen holders consist of 0.010 inch diameter constantan wires extending through cupro-nickel tubes

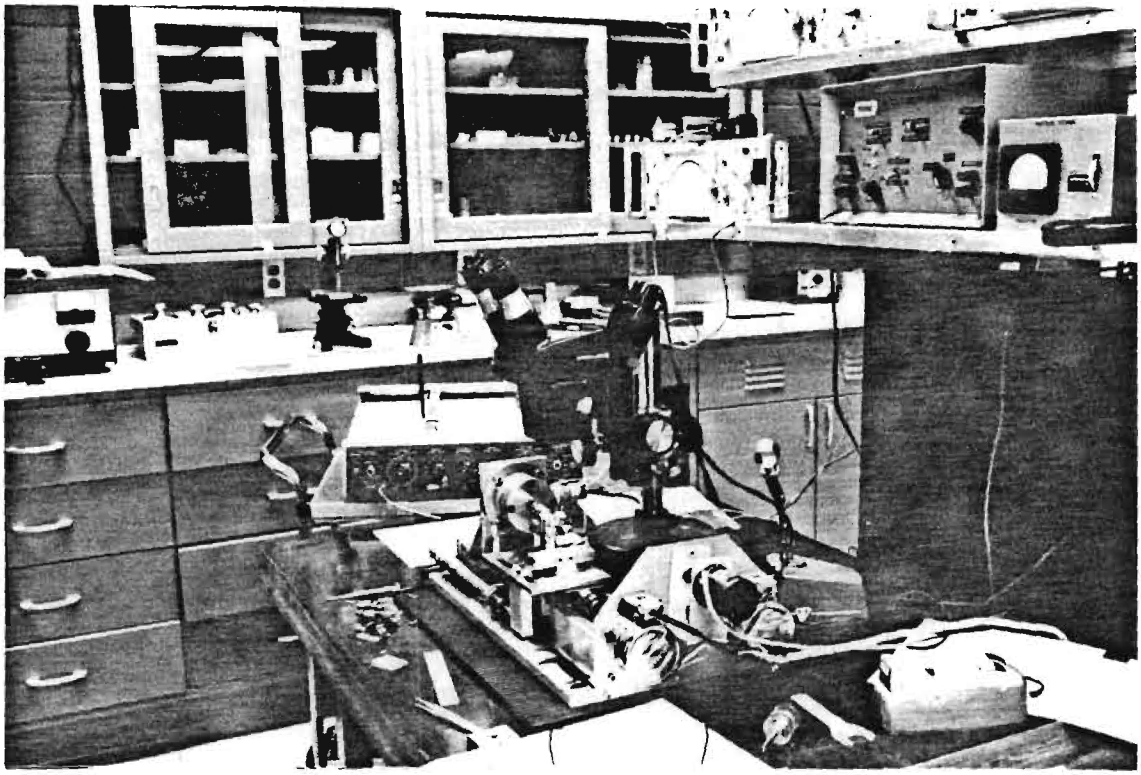

Figure 4. Photograph of Micromechanics Testing Apparatus.

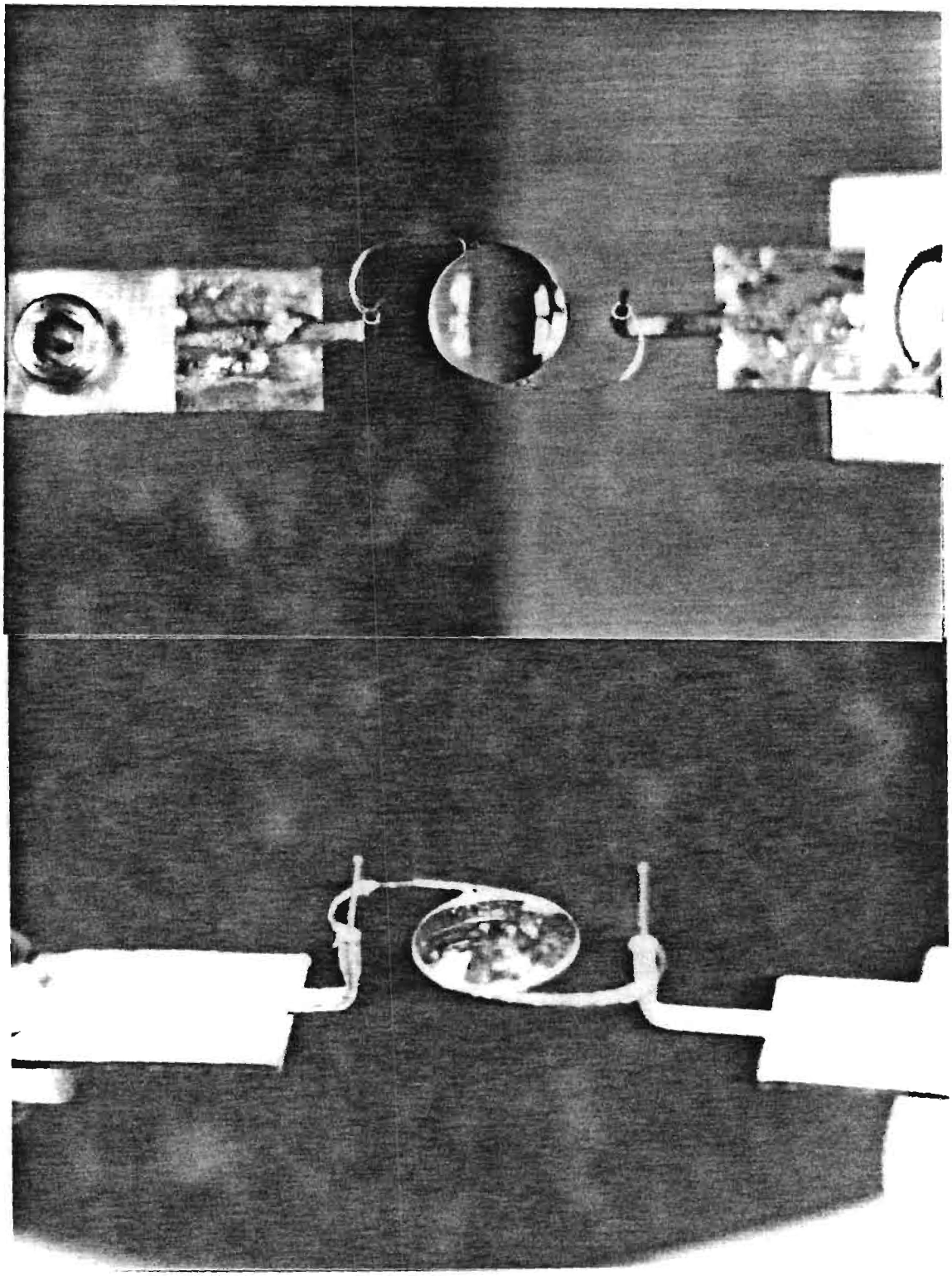

Figure 5. Photographs of Diagonal Compression Test Fixtures.

which were then flatened and soldered to brass tabs. An initial effort at attaching the loops to wires via a wax or glue was judged to be less precise. A photograph showing the test fixtures attached to the differential transformer force transducer is shown in Figure 6. However, the initial diagonal compression runs showed that the more sensitive strain gage transducer shown in Figure 7 was better suited for the force range of interest. (The photographic exposure of the specimen in Figure 7 was not clear due to the microscope illuminating light brightness. The photograph in Figure 6 was included in the report to better illustrate fixture attachment to the transducer.)

The microscope was used to observe possible movement of the lens body as the loops were compressed. Comments concerning individual lenses are included in Table I. In most cases one loop compressed faster than the other such that the support fixture contacted the lens body first on that side. The effect is seen by the discontinuous change in slope on the force-displacement curve shown in Figure 8. The stiffer loop continued to compress until the other support fixture contacted the lens as indicated by a abrupt force increase.

Sometimes the lens body deflected out of the plane which includes the two loops and the flat side of the lens. A close-up photograph showing the maximum deflection of a lens body directly down is included as Figure 9. The compression force was greatly reduced when a lens deflected out of the unstressed loop-flat lens surface plane.

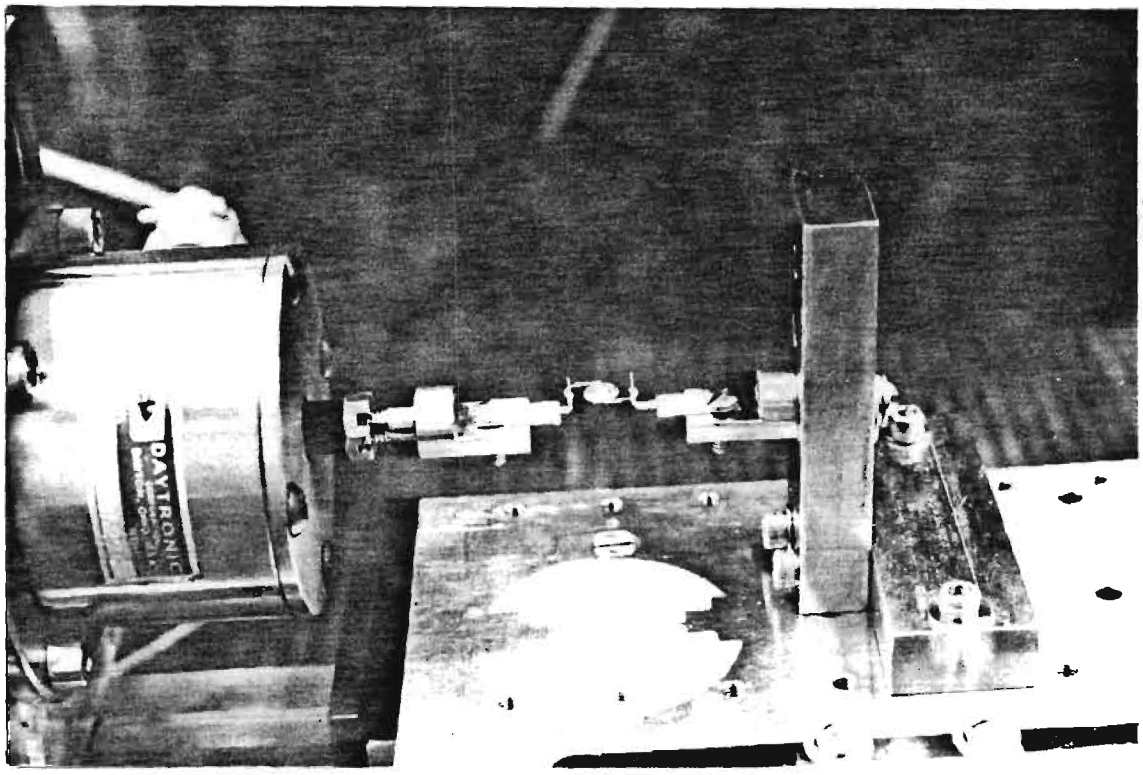

Figure 6. Diagonal Compression Test Fixtures Attached to Differential Transformer Load Cell.

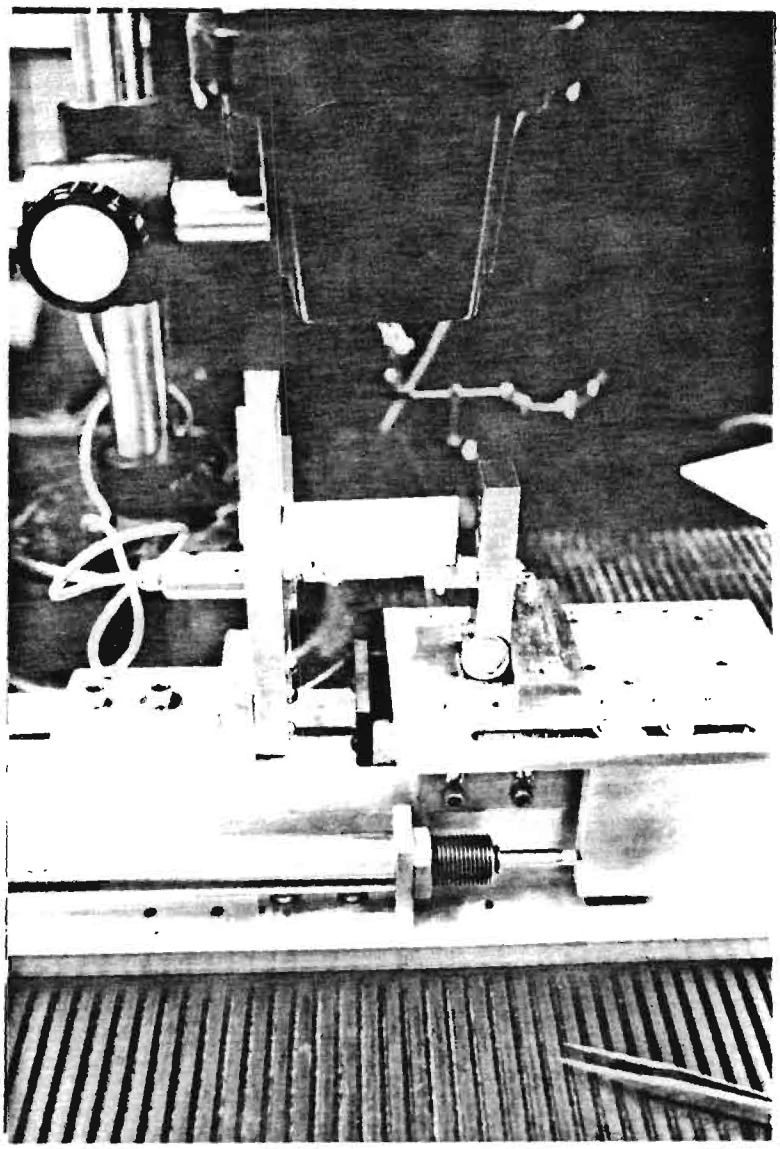

Figure 7. Diagonal Compression Test Fixtures Attached to Strain Gage Transducer as Employed For Measurements.

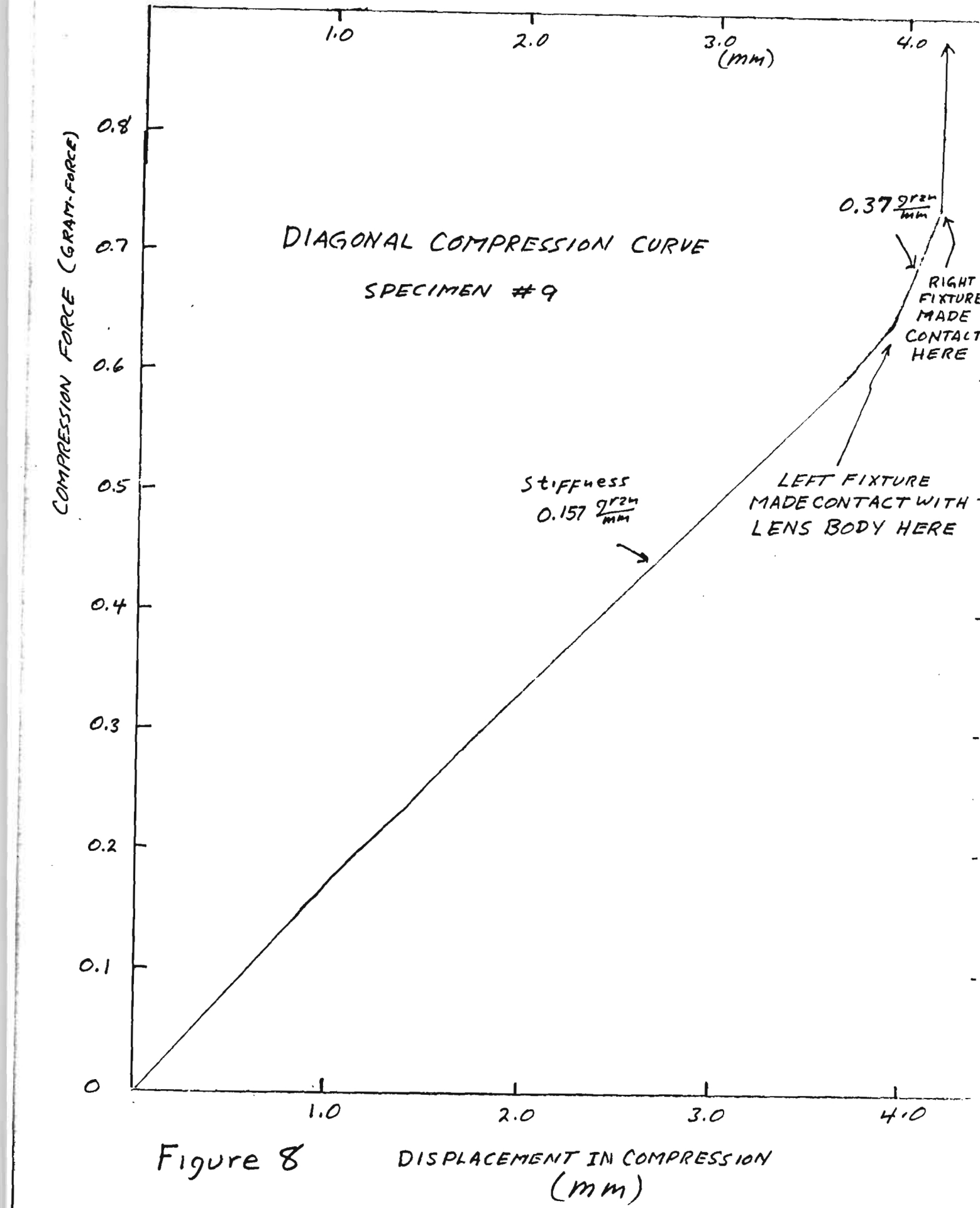
DIAGONAL COMPRESSION CURVE
SPECIMEN #9
COMPRESSION FORCE (GRAM-FORCE)
0.8
0.7
0.6
0.5
0.4
0.3
0.2
0.1
0
1.0
2.0
3.0
4.0
(mm)
0.37 gram/mm
RIGHT FIXTURE MADE CONTACT HERE
Stiffness
0.157 gram/mm
LEFT FIXTURE MADE CONTACT WITH LENS BODY HERE
DISPLACEMENT IN COMPRESSION
(mm)

Figure 8

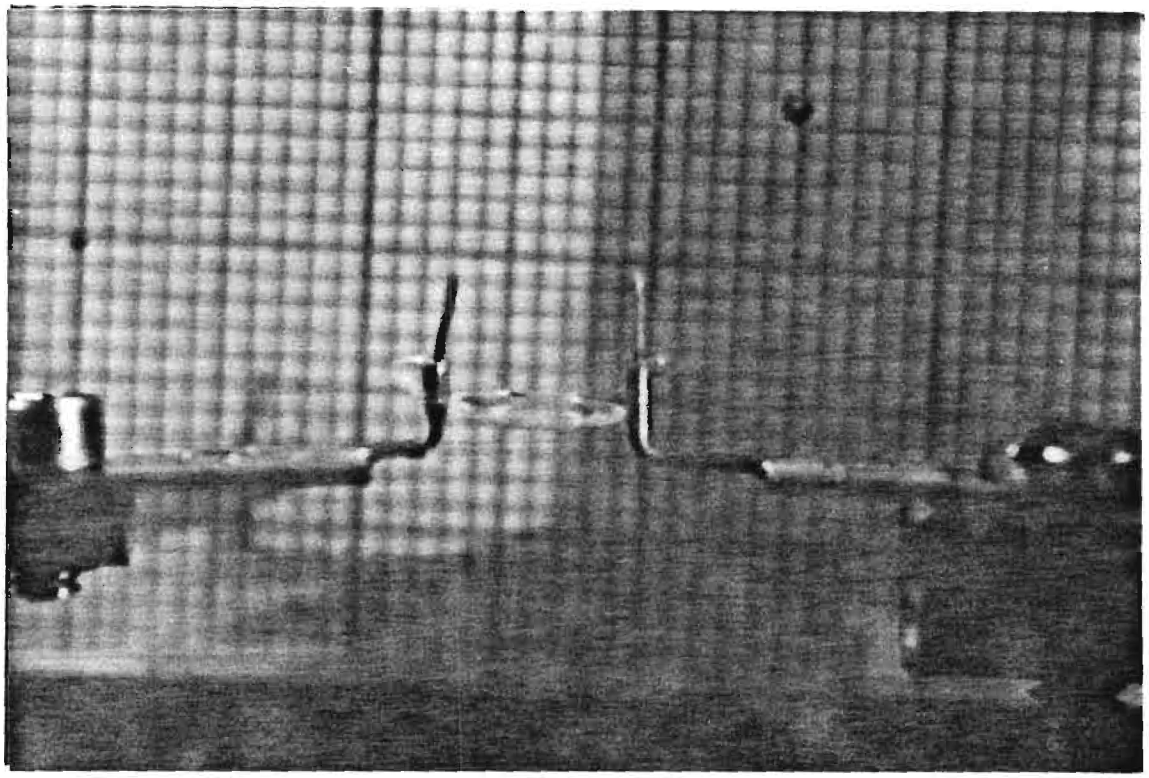

Figure 9. Side View of Diagonally Compressed Lens Which Dropped Significantly Below Plane of Unstressed Lens.

The loop tensile strength fixture arrangement involved several modifications before the simple grips shown in Figures 10-13 were concluded. Attachment to the loop is critical since a non-perfect alignment might cause a loop to break at a lower value than it other wise would. A heat sensitive wax, which is often used here for fiber attachments, was not sufficiently strong so that Eastman 910 was employed for loop attachment. The lens body was then gripped by a brass clamp fitted with neoprene pads. The loop is shown attached by the Eastman 910 to a brass tab in Figure 10. The brass tab is mounted to a swivel grip fixture developed here some years ago. The swivel grip shown attached to the force transducer in Figure 11 allows the tab to tilt in any direction during stressing to accommodate the unavoidable slight mounting misalignment. Figure 12 shows the lens body lying with its flat surface on the lower pad of the clamp with the lens, the lower clamp pad, the tab and the force transducer axis all in the same plane. Figure 13 shows the clamp tightened down on the lens ready for stressing.

The vertical compression, or shear stress test configuration was achieved by fabricating the simple fixtures shown in Figures 14-17. The two lens loops were gripped in viton faced pads made tight by the independently controlled screw clamps shown in Figure 14. This clamp was dismounted from the testing machine and oriented with the pad surfaces horizontal for the necessary precision positioning of the lens prior to tightening the loop grips. The loop clamp was then mounted on the moving stage of the testing machine as shown in Figure 15. Contact was made to the lens by the force transducer through a stainless steel screw with its head ground flat. Adhesives were initially applied to the screw head for bonding to the lens

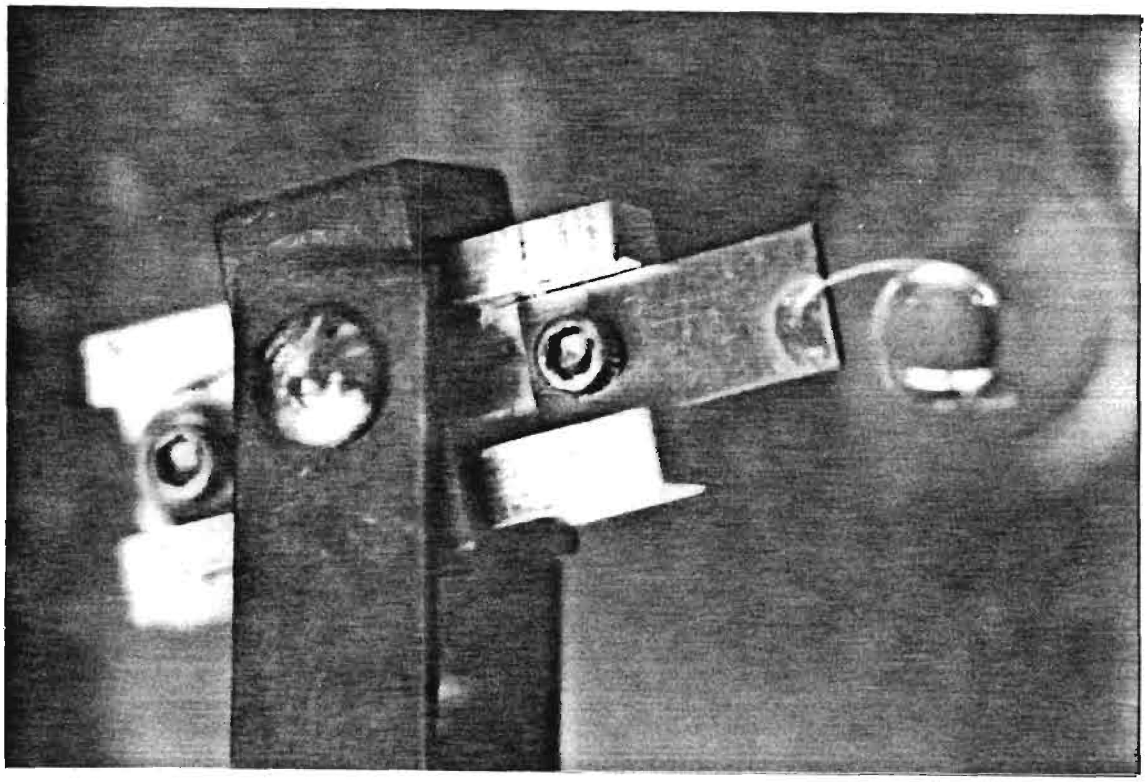

Figure 10. Loop Tensile Test: Loop Attached to Brass Tab and Swivel Grip.

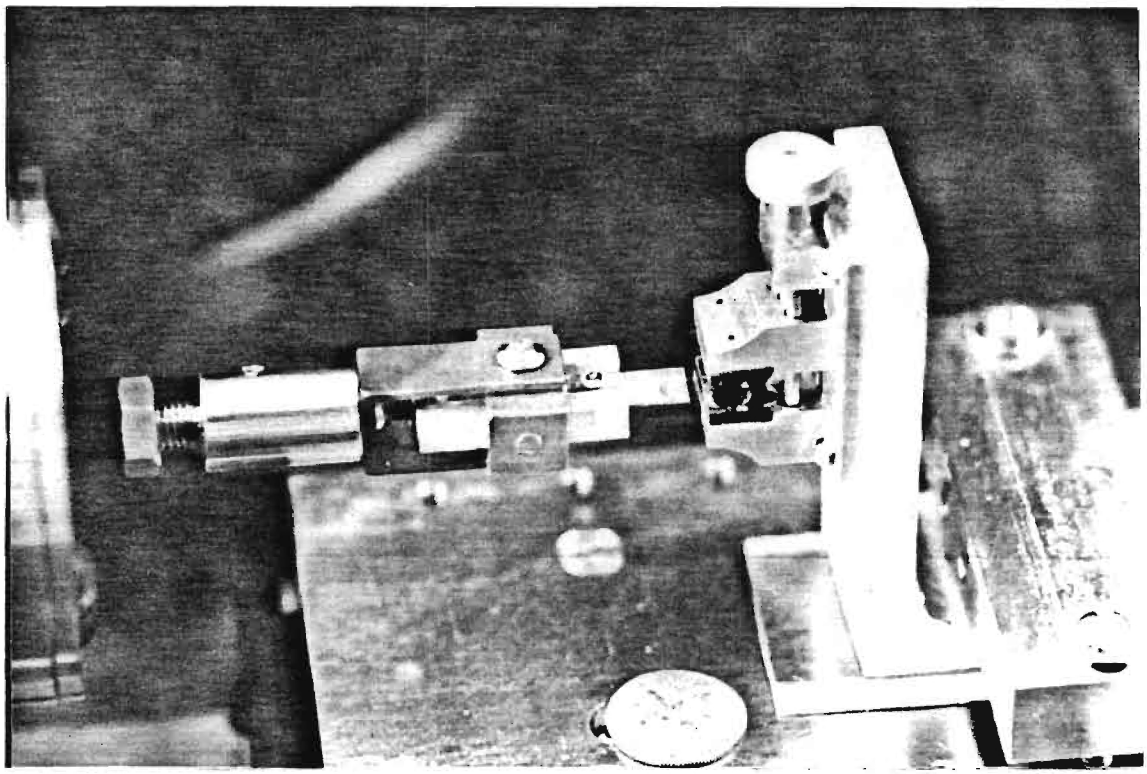

Figure 11. Swivel Grip Oriented With Lens in Clamp.

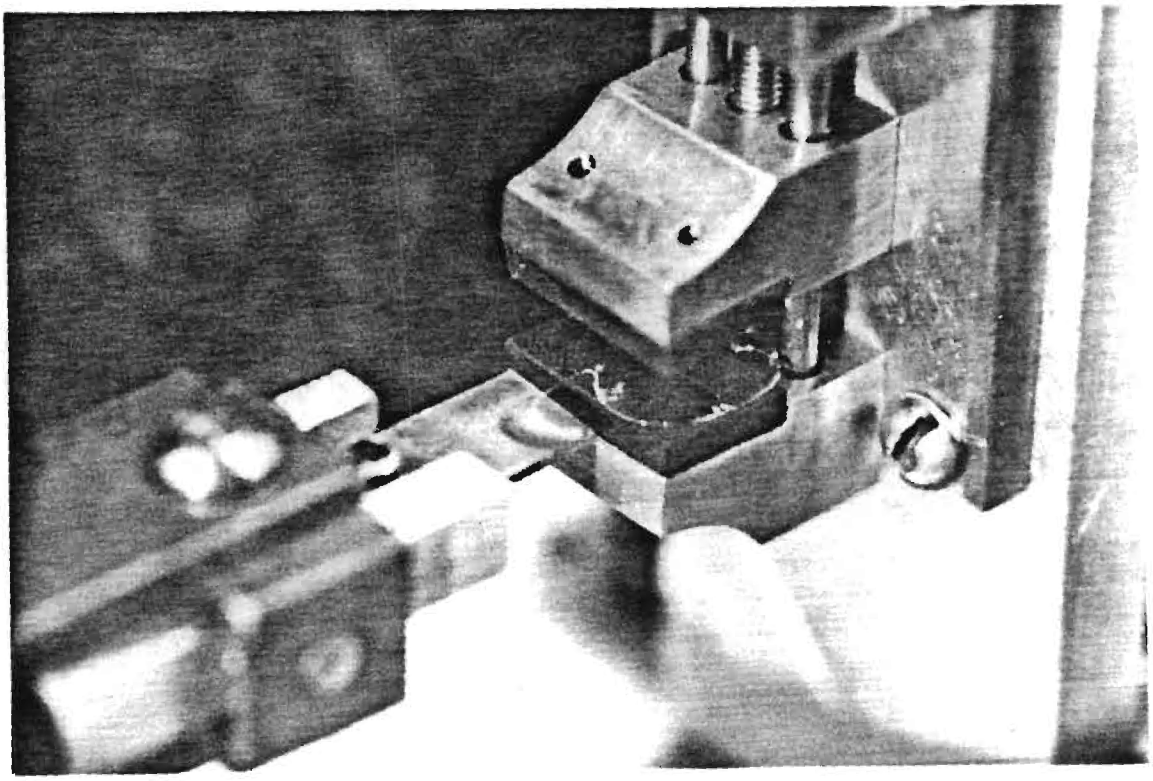

Figure 12. Close-up View Of Lens Clamp For Tensile Test.

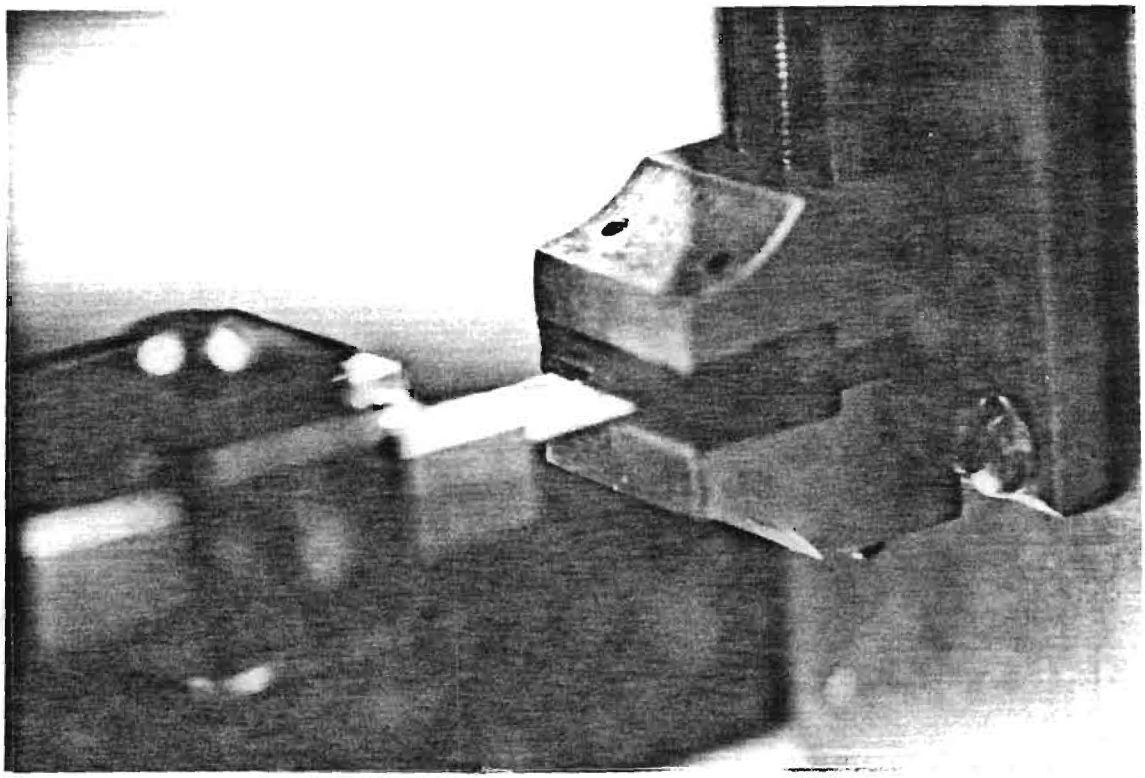

Figure 13. Clamp Tight and Ready For Loop Tensile Test.

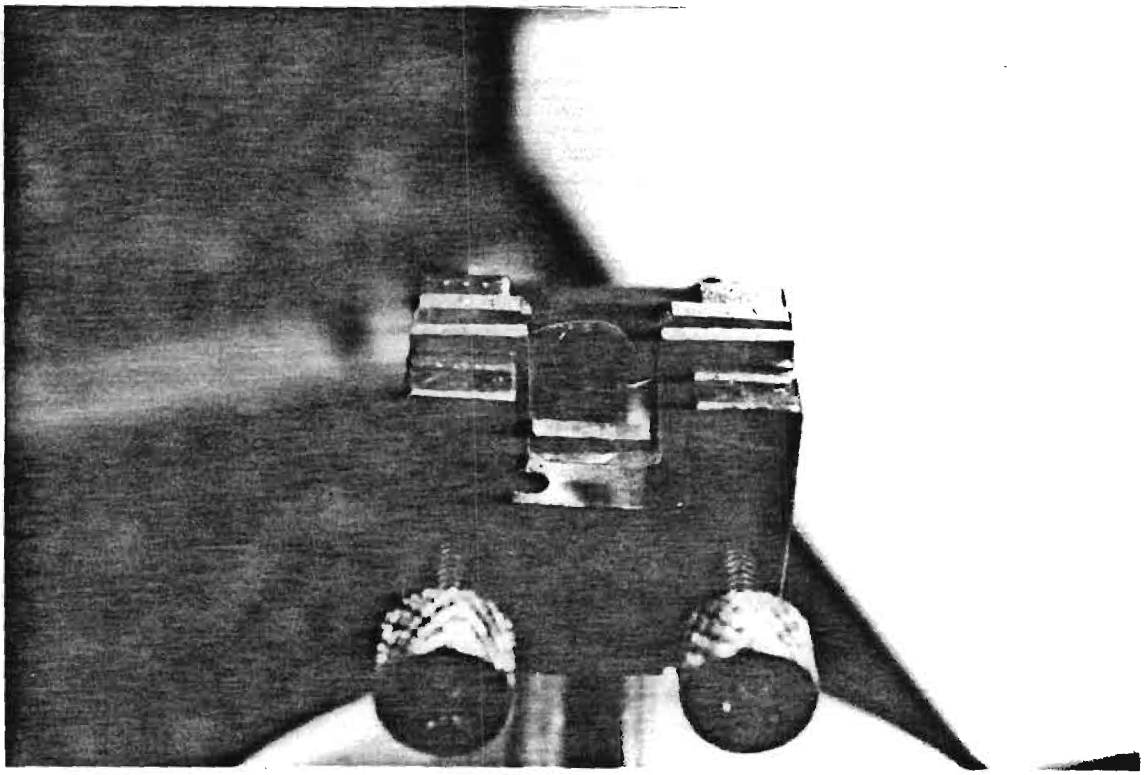

Figure 14. Loop Clamps for Compressive Shear Test.

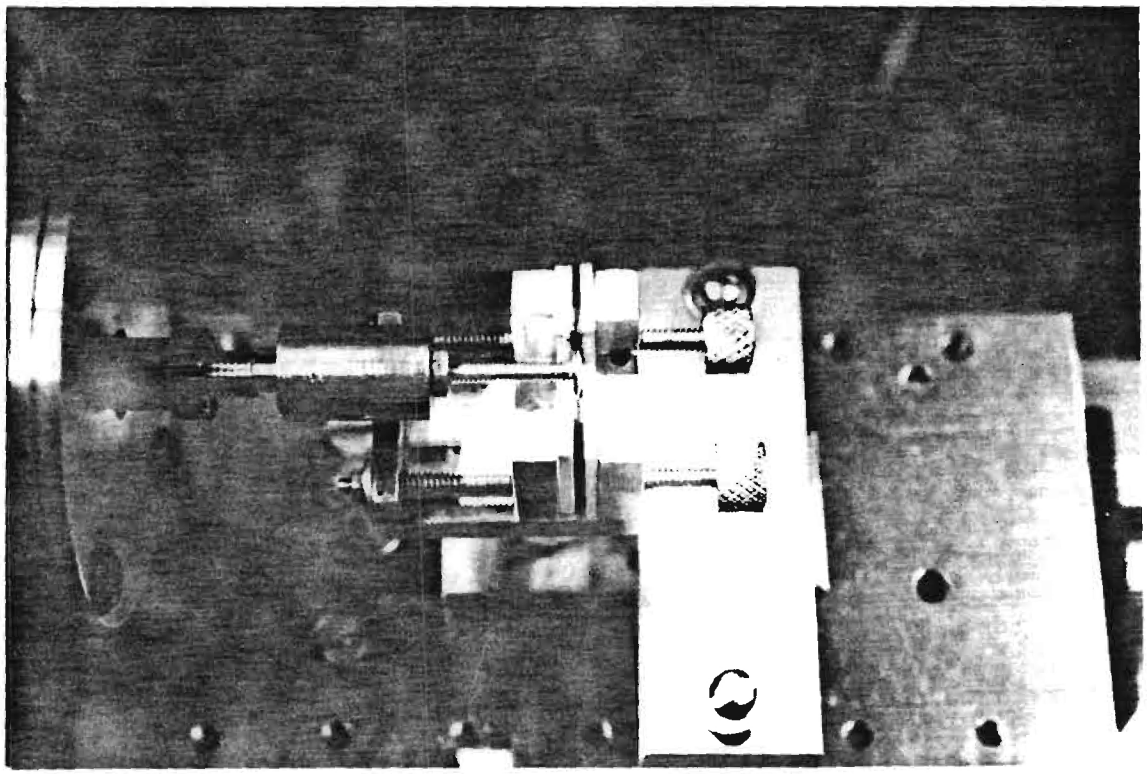

Figure 15. Top View of Transducer Probe in Contact With Unstressed Lens for Compressive Shear Test.

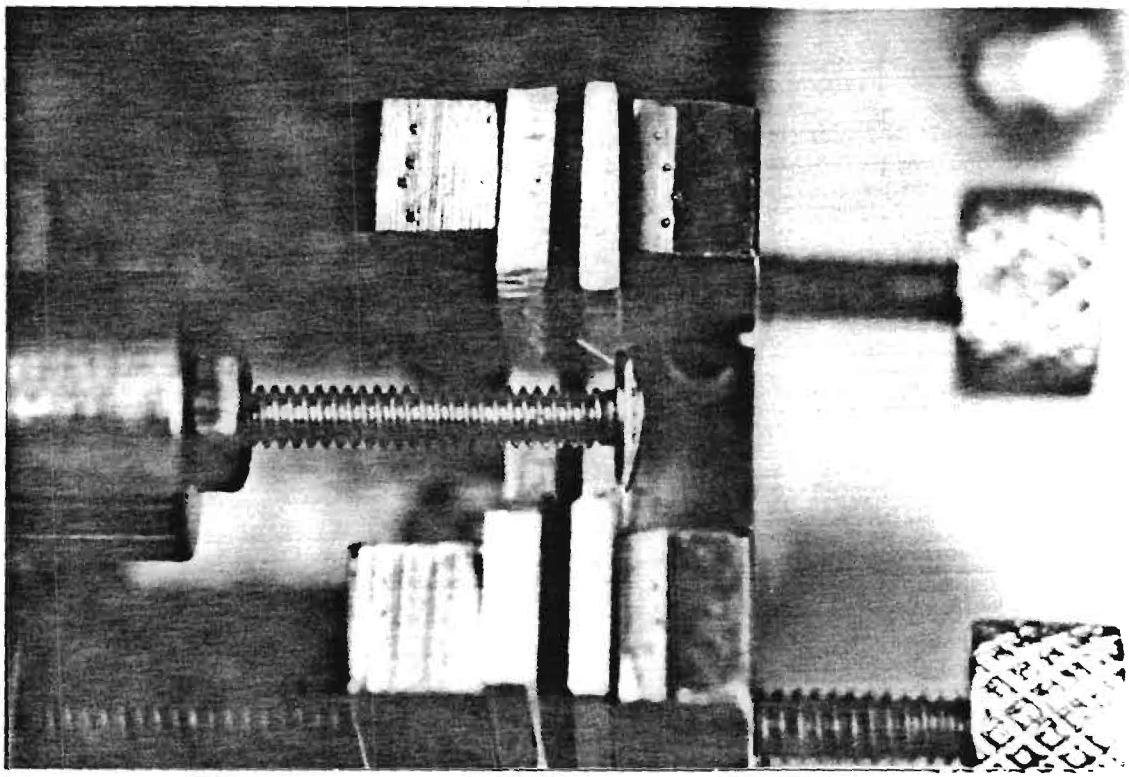

Figure 16. Highly Stressed Lens in Shear Compression With Probe Pushing Against Plain Side of Lens.

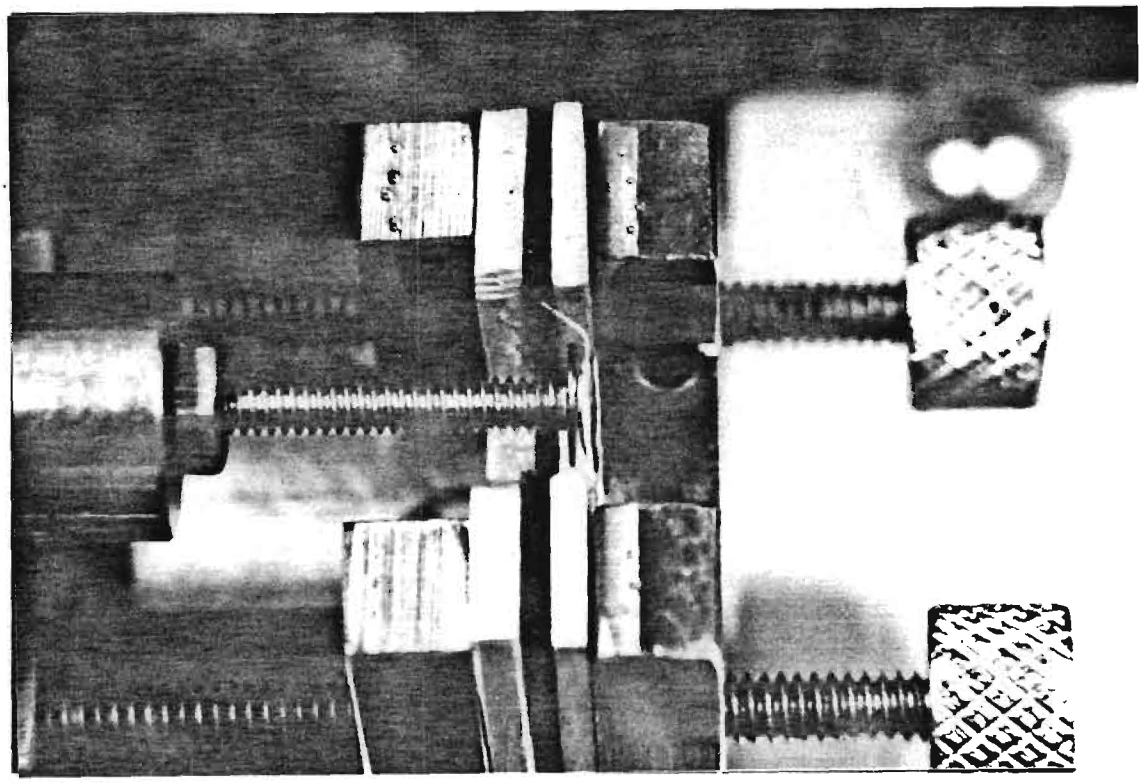

Figure 17. Highly Stressed Lens in Shear Compression With Probe Pushing Against Convex Side of Lens.

body but were found not necessary. Apparently precision positioning of the test fixtures was sufficient to produce uniform elongation of the two loops.

It had been requested that we shear stress half the loops from the planar side of the lens and half from the convex side. Lenses stressed to near fracture for each orientation are shown, respectively, in Figures 16 and 17.

Results

Fifteen lens specimens were tested in each of the deformation modes discussed above. The diagonal compression results are summarized in Table I. It was understood that only the loop compression was important. Therefore the test machine was cut off as both fixtures made contact with the lens body. The sensitive transducer needed for the loop deflection immediately registered such contact by a sudden vertical deflection of the X-Y recorder pen. If one loop was slightly weaker than the other, the lens body made contact with the fixture first on that side as indicated by the increased slope of the force-displacement curve already shown in Figure 8. The slope of this curve is a measure of the spring stiffness of the lens loops at any stage in the loop compression. A second entry was made in the stiffness coefficient column of Table I which corresponds to compression of the stronger loop where contact was made with the other side of the lens sufficiently early to permit measurement of a slope. In each case, the second stiffness coefficient was more than twice as large as the first as would be expected since this region is for the stronger loop alone.

The curve shown in Figure 18 is for a lens with significantly reduced compression force and stiffness coefficient. Visual observations during

Table I

DIAGONAL COMPRESSION

SPECIMEN	MAXIMUM COMPRESSIVE FORCE (gram-f)	MAXIMUM COMPRESSION (mm)	STIFFNESS COEFFICIENT (gram/mm)	VISUAL OBSERVATIONS
1	0.54	4.02	0.16	Highly Stable; Defl. < 0.1 mm
2	0.29	3.62	0.076	Stable in Plane (< 0.1 mm) Vert. 0.8 mm
3	0.66	4.24	0.15	Touch First on Left, Stable
4	0.28	3.56	0.065, 0.17	Right Touched Much Sooner, Lens Body Deflected Down (pictures)
5	0.18	3.94	0.044	Uniform in plane (< 0.1 mm defl.) Slightly Down
6	0.615	4.13	0.150	Highly Uniform (< .1 mm) No Vertical Defl., Touched at Same Time
7	0.072	3.8	0.019	Left Loop Buckled Badly (photos)
8	0.74	4.13	0.16, 0.365	Uniform, No Planar or Vert. Defl.; Left First
9	0.74	4.13	0.157, 0.372	Planar Back to Front ≈ 0.5 mm, No Vert.
10	0.572	3.85	0.121, 0.292	Left First; Slight (0.2 mm) Vertical Defl.
11	0.235	3.87	0.067	Right First; Left Vert. Defl. Down (< 1 mm)
12	0.725	4.04	0.154, 0.363	Right; No Vert. or Planar Defl.
13	0.692	4.10	0.141, 0.349	Left First; No Vert; Back-to-Front 0.5 mm
14	0.37	4.19	0.070, 0.182	Right First; Small Vert. (.2 mm) Right Only
15	0.41	4.00	0.094, 0.21	Left First; Right Drop .2 mm, Left Drop 0.1 mm

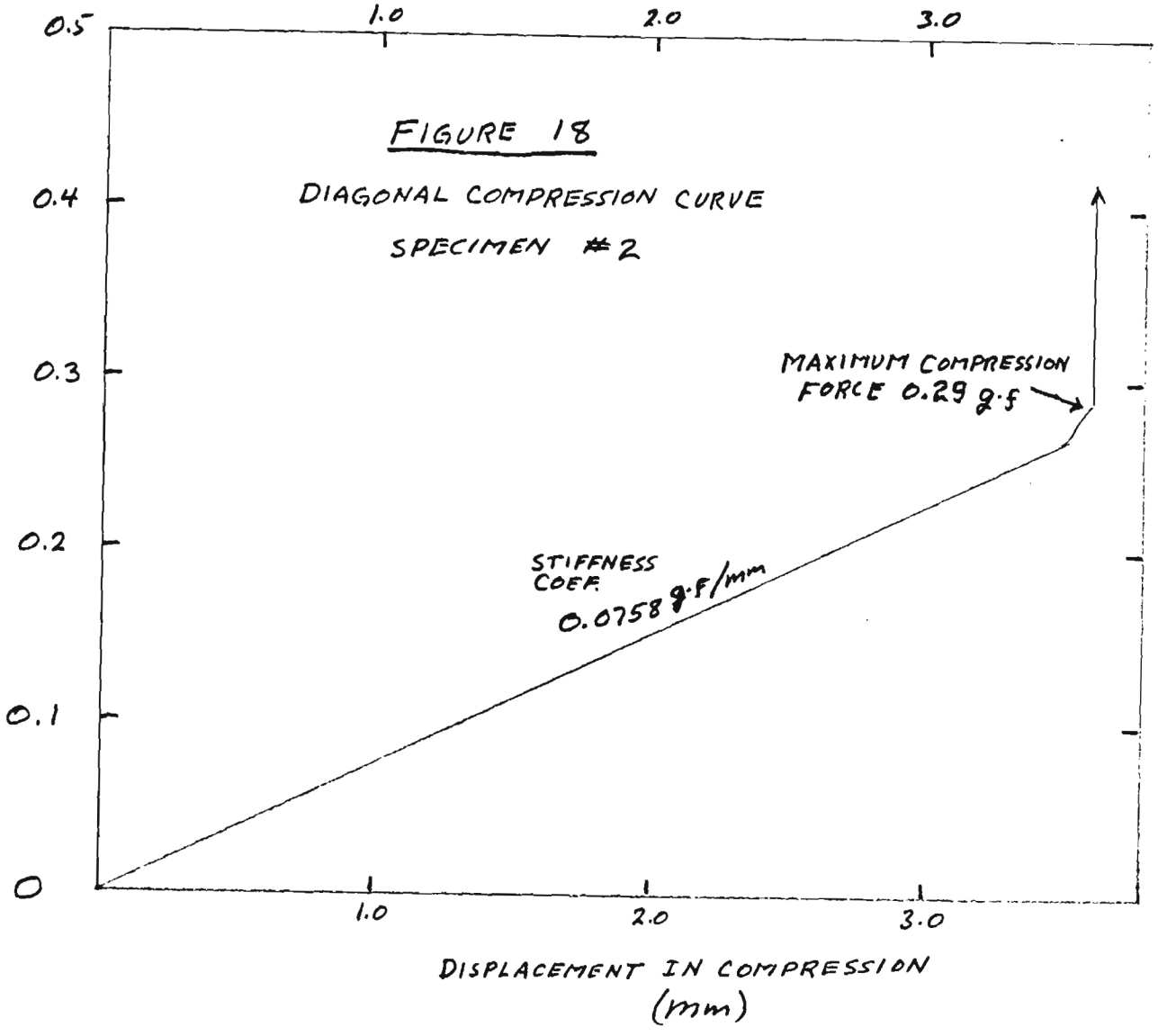

FIGURE 18

DIAGONAL COMPRESSION CURVE

SPECIMEN #2

deformation indicated that the lens body deflected downwards and out of its original plane as the loops were compressed. Most of the lenses were very stable viewed from above during diagonal compression with a slight rotation of the lens body within the lens plane as deformation increased. The curves were mostly linear for all lenses indicating the lens loops compressed according to Hook's Law. Those lens which deflected out of the unstressed lens plane indicated a greatly reduced stiffness coefficient. Whereas the stable lenses yielded stiffness coefficients of 0.14 to 0.16 g-f/mm, those which deflected out of the lens plane were as small as 0.06 or less. A weaker loop could cause movement of the lens body perpendicular to the axis of compression deformation. This did occur in some, but not all, cases. Fixtures could be fabricated which would restrict the lens body to the unstressed plane. However, it was understood here that knowledge of free deflection of the lens body during diagonal compression was part of the information needed to evaluate lens performance. In addition, such a fixture would have to be evaluated carefully to insure that possible small friction interactions with the restricting surface did not alter the compressive force data.

The loop tensile break-strength measurements were made using one loop at a time as suggested by Mr. Johnson. The fixture design discussed earlier and shown in Figure 2 allows the loop to be stressed along an axis tangential to the lens circumference at the point where the loop joins the lens body. A typical force-elongation curve for a loop tensile test is shown in Figure 19. The fracture strengths and elongation at fracture for the loop tensile specimens is provided in Table II. Specimen 15 suffered

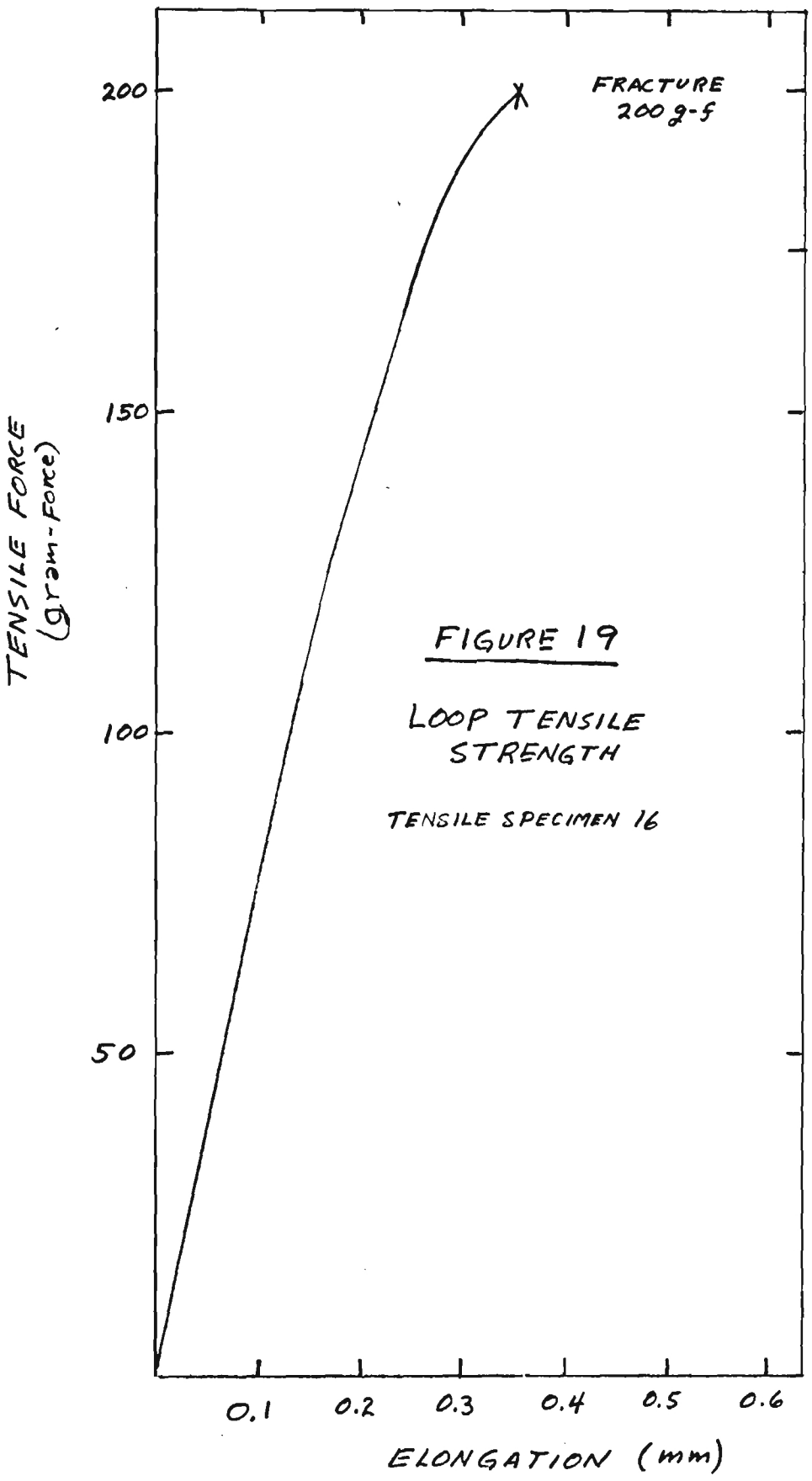

FIGURE 19

LOOP TENSILE STRENGTH

TENSILE SPECIMEN 16

Table II

LOOP TENSILE STRENGTHS

SPECIMEN NUMBER	FRACTURE FORCE (gram/force)	ELONGATION AT FRACTURE (mm)
1	210	0.44
2	123	0.68
3	185	1.16
4	262	0.64
5	76	0.25
6	138	0.39
7	181	0.38
8	207	0.48
9	77	0.24
10	105	0.27
11	132	0.24
12	180	0.32
13	268	0.36
14	78	0.33
15	[162 (max)]	-
16	200	0.35
Averages	161	0.435

failure in the adhesive at the indicated stress level so that an additional specimen was prepared and tested.

Most of the loop tensile fractures occurred near the tab adhesive attachment. This fact bothers experienced mechanical testing personnel. Normally, tensile test specimens are designed with a necked region well away from the grips to insure that the grip attachment itself does not induce premature failure. While the clamp holding the lens body accomplished these desires nicely, there really was no way to achieve even a near ideal arrangement with the loop end of the attachment. As discussed earlier, great care was taken by using the infinitely adjustable grip swivel to minimize misalignment and possible shear at the loop-tab attachment point. In any case, fracture near the tab should not be surprising since the loop material normally appeared to have a minimum diameter in that region. Only specimen number 5 fractured near the lens body.

Observations were made of the loop material during tensile deformation through the microscope. In each case, crazing of the plastic loop span was noted as the tension increased. This observation is typical of what we normally see while stressing various fiber and thin sheet plastic materials. Shapes of the force-elongation curve were also similar to that normally obtained for plastic fiber specimens. While the fracture forces and elongation at fracture values varied over a wide range, average values for the fifteen specimens are included in Table II.

The so named vertical compression test was initially considered to be a bit of a problem due to the apparent asymmetry of the two loops extending from the lenses. In our discussions, the need for an adhesive was anticipated to keep the lens body straight as deformation of the loops progressed. Subsequent to taking time to let the Eastman 910 adhesive set up for the first lens tested in this mode it was suspected that the adhesive was not needed based on observations during deformation. Indeed, this was the case. Careful alignment made possible with the design of these fixtures resulted in a highly symmetrical shear of the lens body - lens loop configuration as shown in the two photographs of Figures 16 and 17 for lenses stressed to near-fracture. A typical shear force- elongation curve is shown in Figure 20 for the vertical compression tests. Results showing maximum fracture strengths and elongation at fracture are provided in Table III.

The locations of fractures were more randomly distributed between the loop grip and the lens body (but with more at the pads) indicating that the viton pads were quite successful in not adversely influencing the data. Specimen 9 fractured at a force much lower than that of any other lens. This fracture point was located where the loop joined the lens body. Average values for fracture strength and maximum elongation are also seen on Table III, with the values for specimen 9 excluded from the calculations.

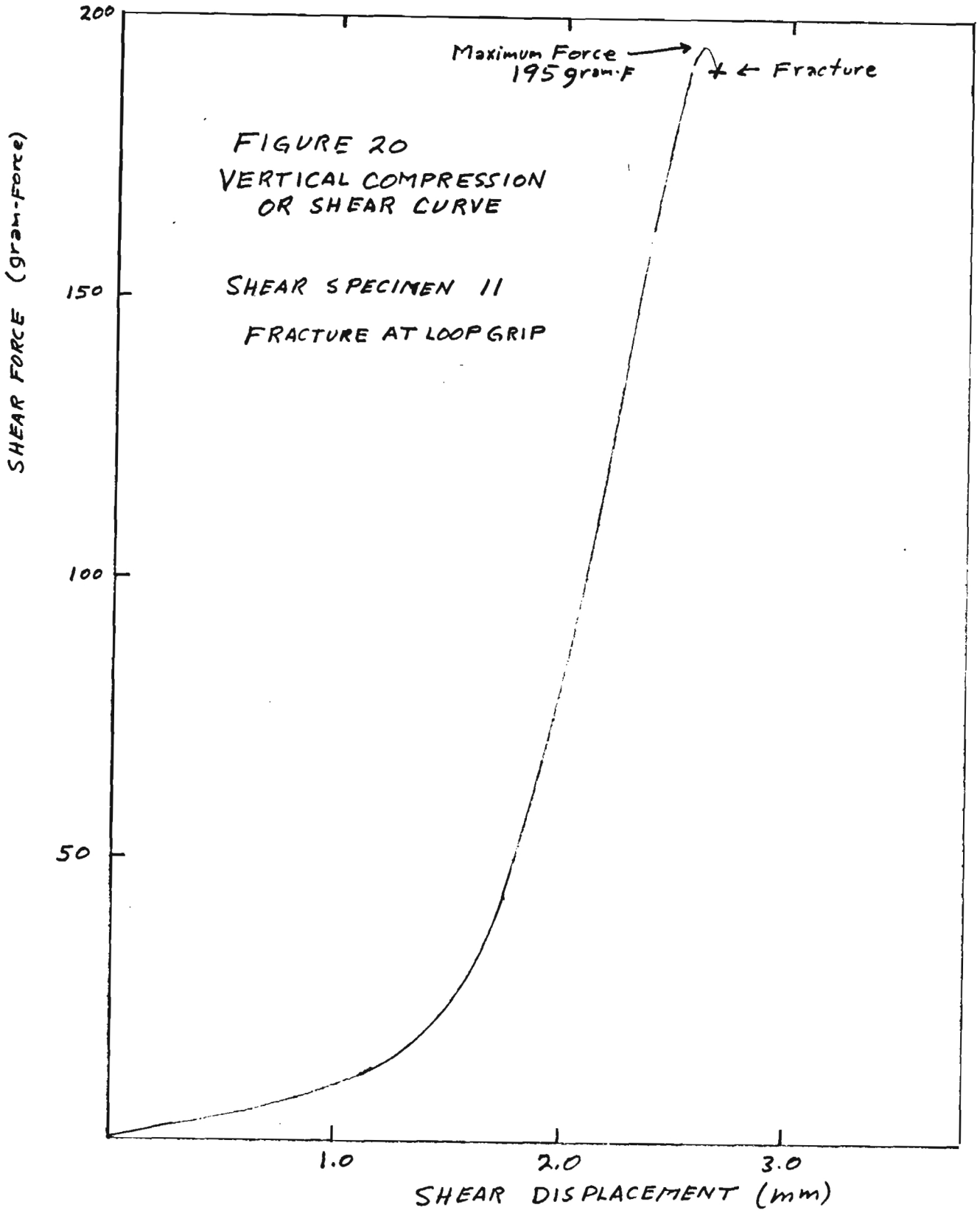
200
150
100
50
SHEAR FORCE (gram-force)
Maximum Force
195 gram-F
← Fracture
FIGURE 20
VERTICAL COMPRESSION
OR SHEAR CURVE
SHEAR SPECIMEN 11
FRACTURE AT LOOP GRIP
1.0
2.0
3.0
SHEAR DISPLACEMENT (mm)

TABLE III

VERTICAL COMPRESSION OR SHEAR TESTS

Specimen	Maximum force (gram -)	Maximum Elongation mm
1	193	3.4
2	221	2.9
3	163	4.1
4	199	4.2
5	185	2.8
6	295	3.5
7	227	2.9
8	182	3.05
9	(20)	(1.3)
10	125	2.4
11	195	2.65
12	250	3.6
13	245	3.1
14	200	2.0
15	133	2.7
Ave (omitting #9)	201	3.1